Application of GRAAL model to the resumption of International Simple Glass alteration

M. Fournier, P. Frugier, S. Gin

Application of GRAAL model to the resumption of International Simple Glass alteration

Maxime Fournier, Pierre Frugier, Stéphane Gin

SUPPLEMENTARY INFORMATION

Supplementary Note 1 Assumptions for modeling zeolites nucleation-growth

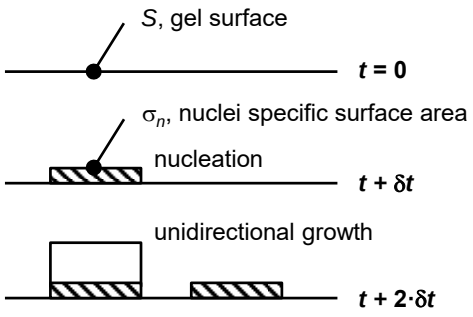

Supplementary Figure 1: In the proposed approach, nucleation occurs at a constant rate on the gel surface area (glass surface area). The nuclei surface area available for zeolites growth is therefore proportional to the time t: $S_c(t) = \sigma_n \cdot n_n(t)$. The zeolites growth occurs is in a single direction, forming needles.

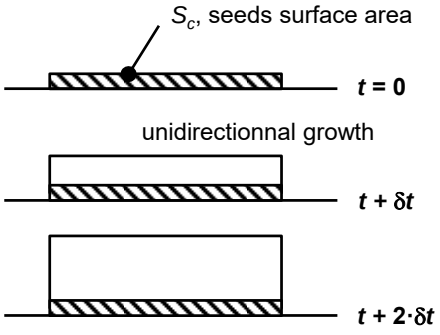

Supplementary Figure 2: In seeded tests, the growth surface area S_c, corresponding to the seeds surface area introduced into the medium at the initial time, is independent of time. The seeds growth is represented by the unidirectional growth of a set of needles.

Supplementary Note 2 Gel description in an alkaline environment

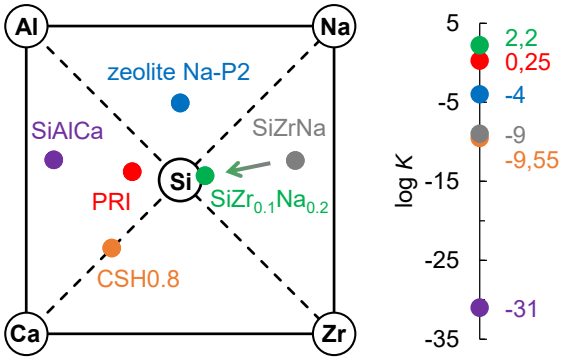

Supplementary Figure 3: In order to integrate the RA phenomenon to the GRAAL model, a new gel composition domain was defined. This domain integrates a passivating (PRI) and three non-passivating end-members (SiAlCa, SiZrNa, and $SiZr_{0.1}Na_{0.2}$). Two secondary phases (Na-P2 zeolites and CSH0.8) also play a role in controlling the activities in solution.

	Phase controlling activity during	
Element	**the *plateau* stage**	**the *RA* stage**
Al	SiAlCa (NPEM)	zeolite Na-P2 (PII)
Ca	CSH0.8 (PII)	CSH0.8 (PII)
Si	PRI	$SiZr_{0.1}Na_{0.2}$ (NPEM)
Zr	SiZrNa (NPEM)	$SiZr_{0.1}Na_{0.2}$ (NPEM)

Supplementary Table 1: Amorphous layer end-members are constructed to ensure the control of Al, Ca, Si, and Zr activities before and during a RA. Activity control could be ensured by the PRI, the gel non-passivating end-members (NPEM), or the secondary phases (PII). The end-member $SiZr_{0.1}Na_{0.2}$ controls both Si and Zr activities during the RA because it has the stoichiometry of the "final gel" towards which the system tends. Boron activity is imposed by the glass dissolution kinetics and Na activity is imposed by a flux corresponding to NaOH additions used to maintain the pH[1].

Supplementary Note 3 Modeling supplementary results

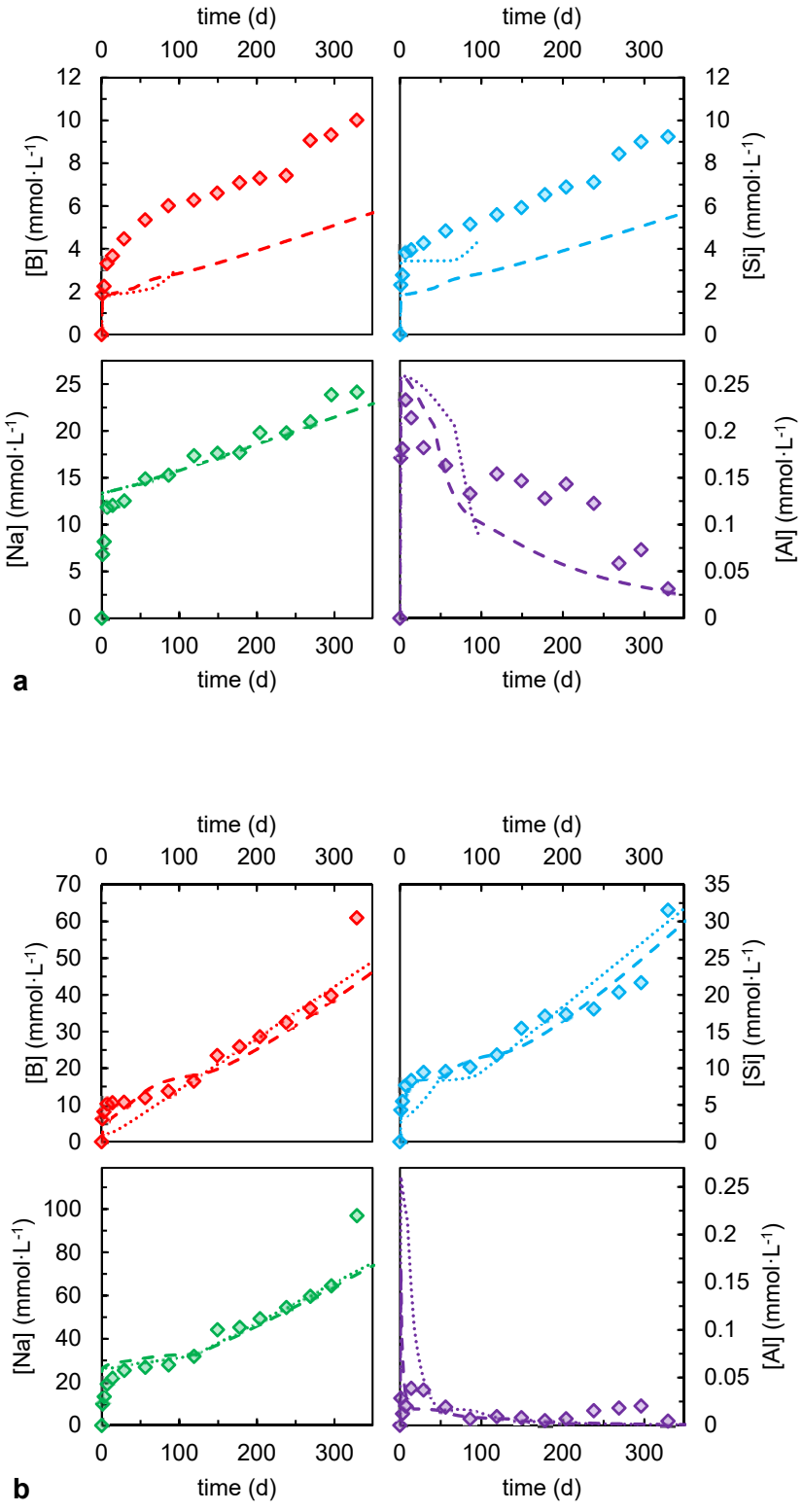

Supplementary Figure 4: Comparisons between modeled and experimental concentrations at **pH 10.1**. Experimental B, Si, Na, and Al [1] (diamonds) and modeled (dashed line for $\beta = 1$ and dotted line for $\beta \to 0$) concentrations in **(a)** unseeded and **(b)** seeded tests conducted at pH 10.1 maintained by adding NaOH in static conditions, at 90°C, S/V = 1,770 m^{-1}.

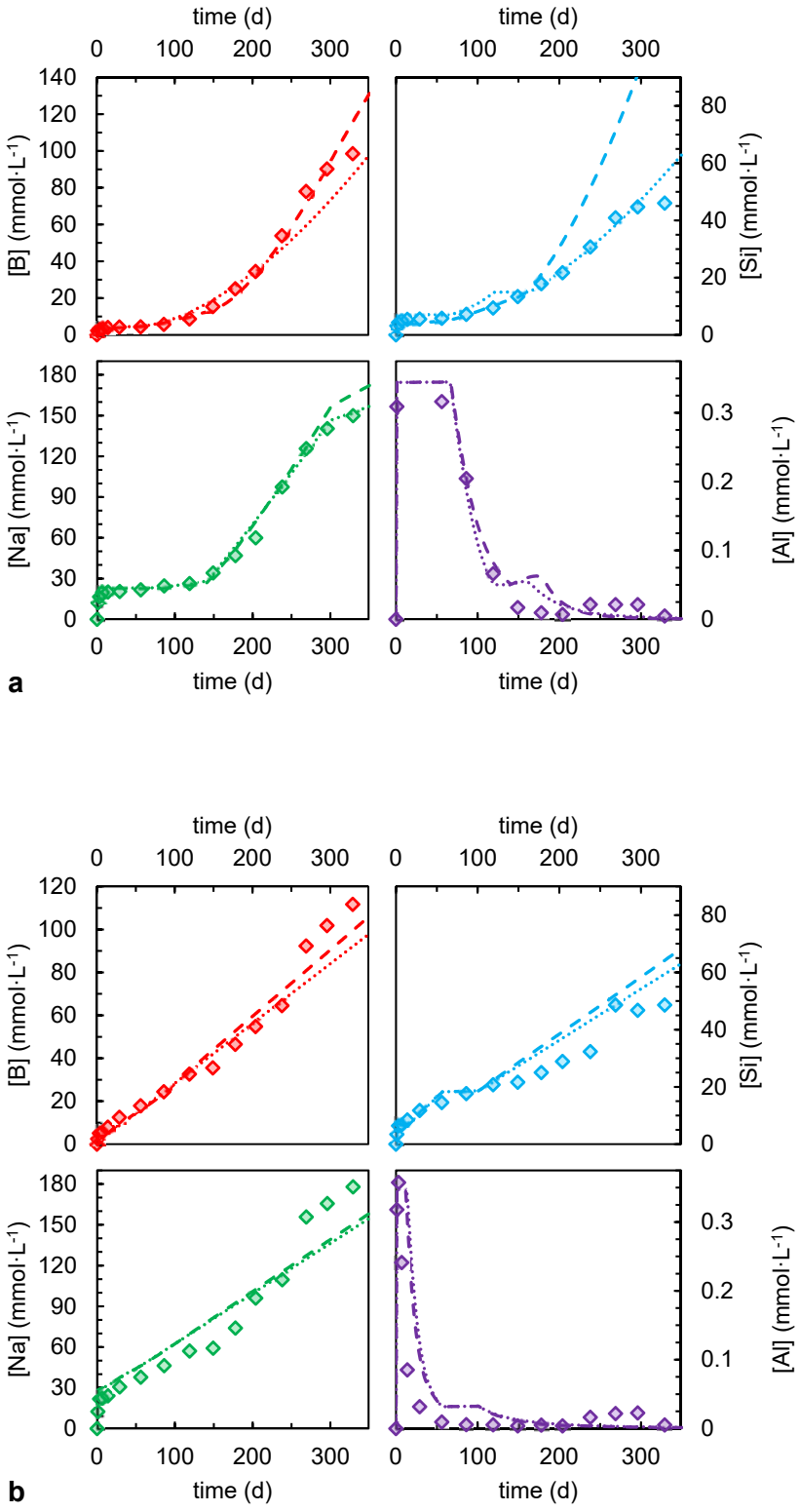

Supplementary Figure 5: Comparisons between modeled and experimental concentrations at **pH 10.4**. Experimental B, Si, Na, and Al [1] (diamonds) and modeled (dashed line for $\beta = 1$ and dotted line for $\beta \to 0$) concentrations in **(a)** unseeded and **(b)** seeded tests conducted at pH 10.4 maintained by adding NaOH in static conditions, at 90°C, S/V = 1,770 m^{-1}.

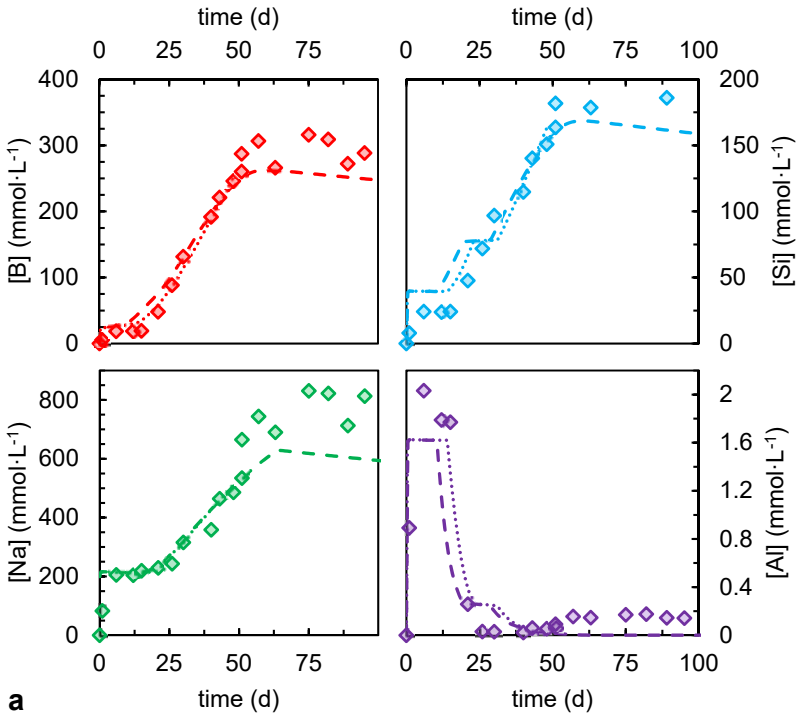

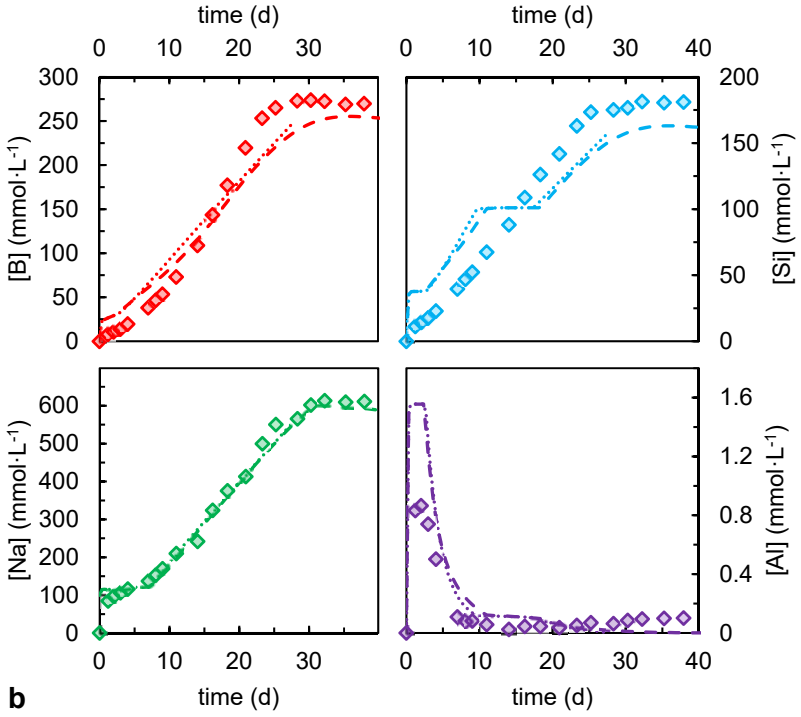

Supplementary Figure 6: Comparisons between modeled and experimental concentrations at **pH 11**. Experimental B, Si, Na, and Al [1] (diamonds) and modeled (dashed line for $\beta = 1$ and dotted line for $\beta \to 0$) concentrations in **(a)** unseeded and **(b)** seeded tests conducted at pH 11 maintained by adding NaOH in static conditions, at 90°C, S/V = 1,770 m^{-1}.

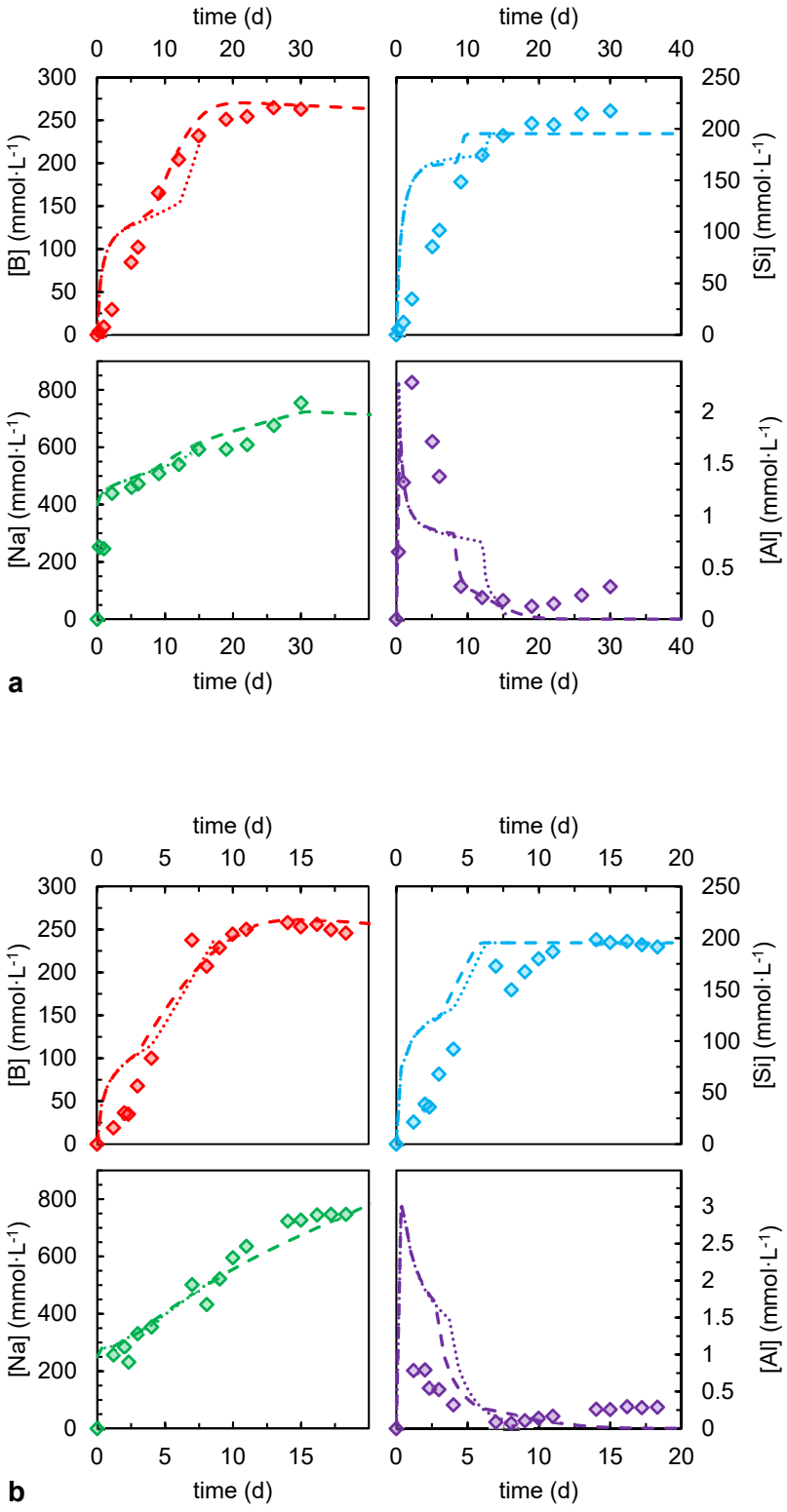

Supplementary Figure 7: Comparisons between modeled and experimental concentrations at **pH 11.3**. Experimental B, Si, Na, and Al [1] (diamonds) and modeled (dashed line for $\beta = 1$ and dotted line for $\beta \to 0$) concentrations in **(a)** unseeded and **(b)** seeded tests conducted at pH 11.3 maintained by adding NaOH in static conditions, at 90°C, S/V = 1,770 m^{-1}.

Supplementary Discussion

The solubility of the Na-P2 zeolite seeds was evaluated by placing synthesized seeds[1] in NaOH solutions of different molarities for one month at 90 °C. The ratio between the seeds "geometric" surface area (0.25 $m^2 \cdot g^{-1}$) and the solution volume was approximately $2 \cdot 10^{-3}$ m^{-1}. The concentrations measured in solution were fairly constant, indicating the early onset of saturation conditions in solution (Supplementary Figure 8). Even at the lowest pH tested (therefore the farthest pH from the synthesis conditions), the dissolution of the seeds was low and the stationary state was reached quickly. The altered zeolite thickness increased with the increase in the pH. Moreover, the Si/Al ratio in solution increase, thus deviating from 1.7, the ratio of the seeds (Supplementary Table 2). The seeds dissolution was not congruent, implying the slow formation of a phase with a stoichiometry different from the starting mineral. Since the maximum equivalent thickness of Si was only 300 nm after one month of leaching, the quantities formed of this (or these) phase(s) remained low, explaining that their identification and characterization could not be completed (not visible by SEM after 330 days at pH ≈ 9).

pH	**9,3**	**9,9**	**10,1**	**10,4**	**10,7**	**11,0**	**11,3**
eTh_{Si}	37	51	69	102	109	197	299
Si/Al	5.0	5.8	5.0	4.5	3.5	3.2	2.2

Supplementary Table 2: Calculation of the equivalent thickness in Si (eTh_{Si}, in nm) of altered zeolite after 29 days and the average Si/Al solution ratio for each pH. The seeds Si/Al ratio is 1.7.

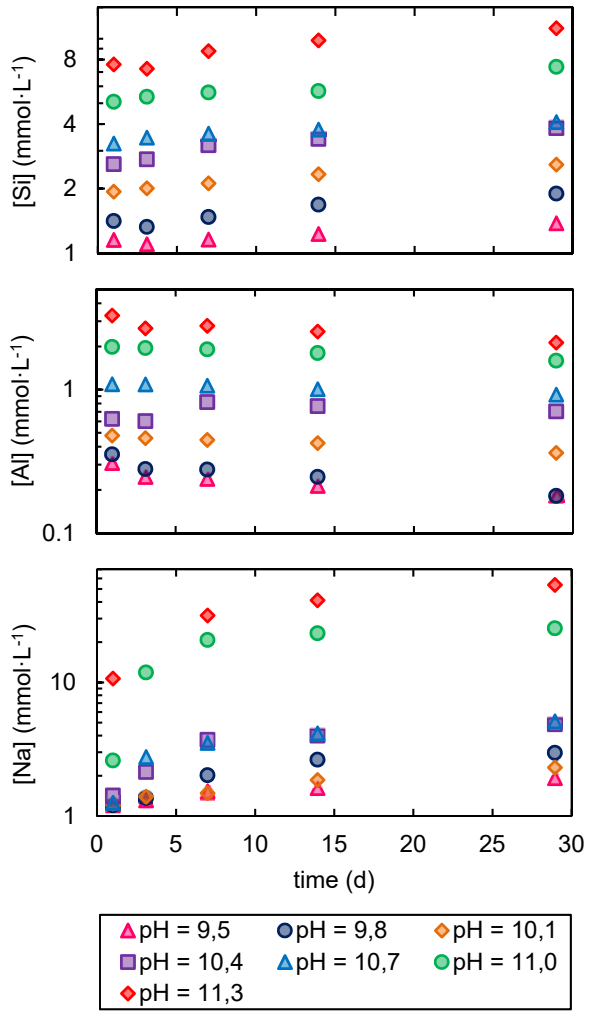

Supplementary Figure 8: Concentrations of Si, Al, and Na measured in solution during the dissolution of Na-P2 zeolite seeds in NaOH solutions of different molarities. The initial sodium concentrations were subtracted.

The solubility constant of the Na-P2 zeolite was calculated using the CHESS code for different pH values. This calculation required the implementation of the following dissolution-precipitation reaction in the database, using a stoichiometry measured elsewhere[1]:

$$NaAlSi_2O_8H_4 + 4\,H^+ = 1\,Na^+ + 1\,Al^{3+} + 2\,H_4SiO_4$$

For all the pH values studied, we calculated a solubility constant value at each sampling time (1, 3, 7, 14, and 28 days respectively). The results obtained were similar for the same pH but varied substantially from one pH to another (Supplementary Figure 9).

[1] Fournier, M. *et al. npj Mater. Degrad.* **1**, 17 (2017).

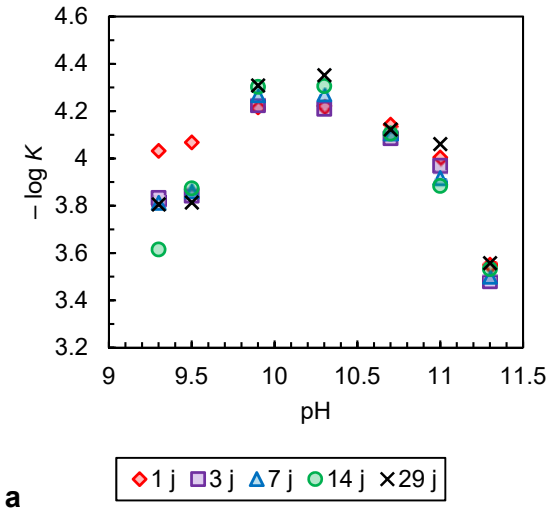

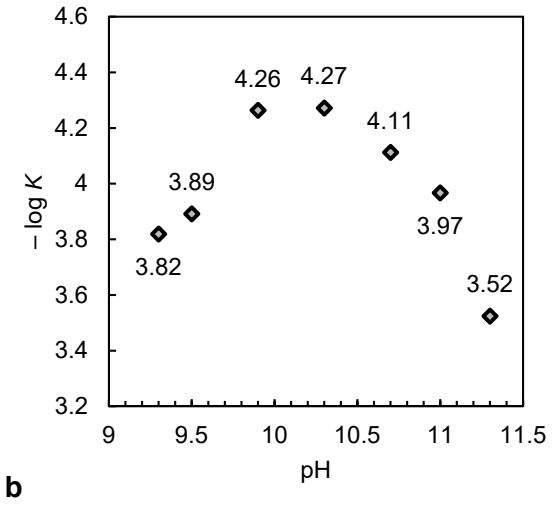

Supplementary Figure 9: Data derived from calculating the solubility constant *K* of the Na-P2 zeolite **(a)** at each sampling time and **(b)** on average for the different studied pH values.

The solubility constant of a mineral does not depend on the pH. The variations observed in Supplementary Figure 9(b) are thus related to the uncertainties associated with log *K* measurements. The average solubility constant ($\log K = -4.0$) reasonably describes the equilibrium between the Na-P2 zeolite and the NaOH solutions (Supplementary Figure 10). This log *K* value was used in the calculations presented in the main text.

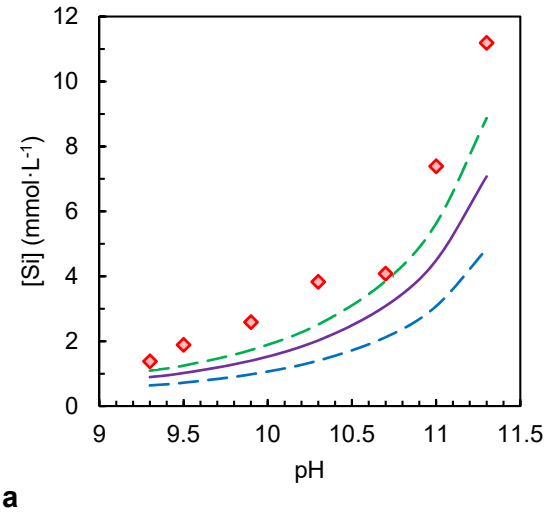

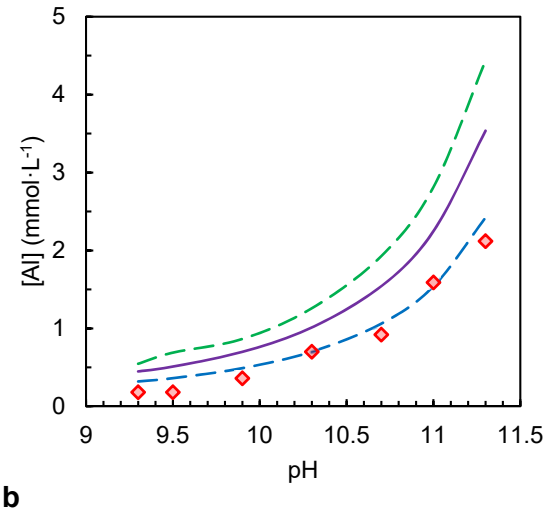

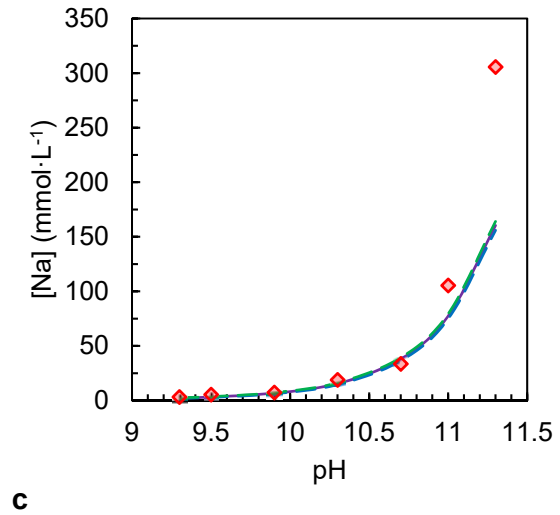

Supplementary Figure 10: Comparison between **(a)** Si, **(b)** Al, and **(c)** Na concentrations measured after 29 days (red diamonds) and those calculated using three solubility constant values for the Na-P2 zeolite: $\log K = -4.0$ (purple line), $\log K_{min} = -4.3$ (green dashed line), and $\log K_{max} = -3.5$ (blue dashed line).